CSAWAC 43 (7) 967–1114 (2015) · Vol. 43 · No. 7 · July 2015

CLEAN

Soil Air Water

Renewables

Sustainability

Environmental Monitoring

7|2015

www.clean-journal.com

WILEY

CLEAN
Soil Air Water

Danlin Zeng
Shenglan Liu
Wanjun Gong
Guanghui Wang
Jianghua Qiu
Hongxiang Chen

Hubei Key Laboratory of Coal Conversion and New Carbon Material, College of Chemical Engineering and Technology, Wuhan University of Science and Technology, Wuhan, P. R. China

Research Article

Effect of Surface Properties of Iron Oxide Sorbents on Hydrogen Sulfide Removal from Odor

Hydrogen sulfide (H_2S) removal is the key issue for the odor control of sewage treatment facilities. In this paper, the iron oxide sorbents with different surface acid–base properties were prepared by acid and base modification. Effect of surface properties of iron oxide sorbents on H_2S removal was revealed by the characterization of surface pH, Fourier-transform infrared spectroscopy, X-ray photoelectron spectroscopy, and solid-state NMR spectroscopy. The results show that the activity loss of the iron oxide sorbent is mainly due to the gradual oxidation of H_2S into elemental sulfur and further into the sulfuric acid and sulfurous acid with time on stream. Meanwhile, the surface basic environment of base-treated iron oxide sorbent significantly increases the H_2S removal activity by suppression the formation of H_2SO_4 or H_2SO_3 during the desulfurization process. Our findings will help us to prepare novel sorbent for more effective H_2S removal from, e.g., odor gas.

Keywords: Desulfurization method; Odor pollution; Surface acidity

Received: April 18, 2013; *revised:* October 16, 2013; *accepted:* November 15, 2013

DOI: 10.1002/clen.201300328

1 Introduction

As a malodorous gas, hydrogen sulfide (H_2S) is harmful to human health, industrial catalysts, and environment [1]. This rotten eggs smell gas can be detected by human in a very low concentration. In addition, high H_2S concentrations seriously affect the nervous and respiratory system of human. Many attentions have been focused on H_2S removal from odor gas arising from sewage treatment facilities as the restrictive emission standards are enacted world widely [2–9]. The removal of H_2S with iron oxide sorbents is a classic and effective desulfurization method due to its advantages of high sulfur removal efficiency, low cost, simple operation, and no secondary waste for additional treatment [10, 11]. Furthermore, it exhibits the ability to remove H_2S completely at ambient temperature and normal pressure. The exhausted sorbent can be easily regenerated by exposing the sample to air. Under such conditions, the ferric sulfide will be converted back into ferric oxide and elemental sulfur and then be recycled for further H_2S adsorption. Therefore, H_2S removal over iron oxide sorbent is probably the most promising way for the control of odor pollution.

As reported by other researchers [12], the surface acidity plays a significant role in H_2S removal reaction. It is found that the acidic surface leads to the formation of sulfur oxides and further to sulfuric acid while the basic surface favors the formation of elemental sulfur and also increases the H_2S removal efficiency. Consequently, surface acidity of the iron oxide sorbent may also greatly influence its sulfur removal activity. But unfortunately, the effect of the acidic property on the catalytic performance and the role of the acid or base sites in this reaction are still poorly known. Hence, it is worthwhile to reveal the relationship between surface acid–base properties and activity of the H_2S removal reaction on the iron oxide sorbents.

In the present work, the iron oxide sorbents with different surface acid properties were prepared by HNO_3 and NaOH modification. Effect of surface properties of iron oxide sorbents on H_2S removal was revealed by the characterization of surface pH, Fourier-transform infrared (FT-IR) spectrometry, X-ray photoelectron spectroscopy (XPS), and solid-state NMR spectroscopy. The influence of surface acidity on H_2S removal was obtained on the basis of our experimental results.

2 Materials and methods

2.1 Sample preparation

Ferrous chloride was the main material for the preparation of iron oxide sorbent. Kaolinite, diatomite, bentonite, and mixed clay were chosen as the additives of the sorbent. Ferrous chloride solution, additive, organic binder, and extrusion aid were blended with water, and followed by stirring, aging, filtrating, and then after extruding, drying at 393 K for 12 h, the iron oxide sorbent was obtained.

For the preparation of acid-treated sample, the dried iron oxide sorbent from above was impregnated with 1×10^{-4} M HNO_3 solution (pH 4) with a solid/liquid ratio of 1:5 for 10 h at room temperature and then the sample was filtered, washed thoroughly with deionized water, dried at 393 K overnight, and then activated at 673 K in the vacuum of $<1 \times 10^{-3}$ Pa for 5 h. For the preparation of base-treated sample, the procedure is the same as above except that the dried iron oxide sorbent was impregnated with 1×10^{-4} M NaOH solution.

2.2 Sample characterization

The pH of the sorbent surface was measured in the following way. 0.4 g dry sorbent powder was added to 20 mL deionized water, and

Correspondence: Dr. D. Zeng, Hubei Key Laboratory of Coal Conversion and New Carbon Material, College of Chemical Engineering and Technology, Wuhan University of Science and Technology, Wuhan 430081, P. R. China
E-mail: zdanly@163.com

Abbreviations: **FT-IR**, Fourier-transform IR; **IR**, infrared; **TMPO**, trimethylphosphine oxide; **XPS**, X-ray photoelectron spectroscopy; **XRD**, X-ray diffraction

CLEAN Soil Air Water

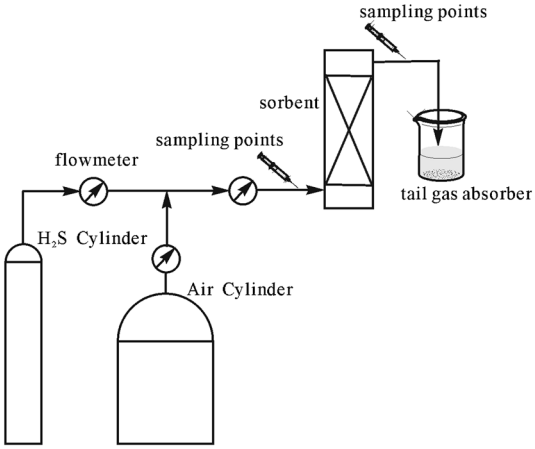

Figure 1. Schematic diagram of the dynamic test.

then the mixture was stirred for 12 h to reach equilibrium. After the mixture was filtered, the pH of the filtrate was measured to obtain the pH of the sorbent surface.

The FT-IR spectra were recorded on Impact 410, Nicolet spectrometer with a resolution of 2 cm^{-1}. Twelve milligrams of each sample were pressed into a self-supported wafer 16 mm in diameter. The wafers were heated at 200 °C in an infrared (IR) cell under vacuum ($<10^{-3}$ Pa) for 4 h before the IR spectra of the samples were measured.

XPS was performed with the EscaLab 210 photoelectron spectrometer using a non-monochromatized Al Kα radiation (1486.6 eV), which was operated at 15 kV and 34 mA.

The solid-state NMR characterization was performed on a Varian Infinityplus-400 spectrometer.

X-ray diffraction (XRD) was performed with a Philips X'PERT-Pro-MPD diffractometer, operating with Cu Kα radiation (40 kV, 30 mA) and Ni filter.

The adsorption of trimethylphosphine oxide (TMPO) was performed as follows: 1 g dehydrated sorbent was mixed with 2 mL CH_2Cl_2 solution containing 0.1 M TMPO in a glove box, and then the mixture was stirred for 3 h by an ultrasonic shaker, equilibrated for 5 h, at last the mixture was evacuated under vacuum to remove CH_2Cl_2 and physorbed TMPO.

The dynamic test was performed to characterize the sulfur capacity of the sorbents. Desulfurization activities were evaluated by a fixed-bed glass reactor of 30 mm in diameter and 300 mm in length at room temperature and normal pressure. The odor gas used in this work is the mixture of moist air (relative humidity 80% at 298 K) containing 1000 mg/m^3 H_2S. The gas flow rate was controlled by flow meters. The H_2S vapor and air were mixed after the flow meters. The space velocity of the mixed gas was 1000 h^{-1}. The exhausted tail gas was washed by a tail gas absorber with 0.1 M NaOH solution. When the H_2S concentration in the exit gas was higher than 50 mg/m^3, the test was stopped, and then the breakthrough sulfur capacity was calculated based on the test time, H_2S concentration, and mass of the sorbent. The concentration of the H_2S was determined by the HP6890 GC with a flame photometric detector. The schematic diagram of the dynamic test is shown in Fig. 1.

3 Results and discussion

Table 1 shows the physical parameters and the surface pH of the sorbents. It can be seen that for the three samples bulk density,

Table 1. Physical parameters and pH of the sorbents

Sorbents	Bulk density (g/mL)	Brunauer–Emmett–Teller surface area (m^2/g)	Porosity (%)	pH
Iron oxide sorbent	0.80	110	42	7.56
Acid-treated sorbent	0.78	100	43	6.20
Base-treated sorbent	0.81	109	39	8.50

surface area, and porosity are almost the same except for their different surface pH. Therefore, the acid or base treatment exhibits crucial effect on the surface pH of sorbents while its physical parameters were almost unchanged. Acid treatment increases the surface acidity of the sorbent while base treatment increases its surface basicity compared with the untreated sorbent.

The XRD patterns of acid-treated sorbent, iron oxide sorbent, and base-treated sorbent are shown in Fig. 2. The XRD spectra exhibits remarkable diffraction peaks arising from α-Fe_2O_3 (at 24.1°, 33.1°, 35.6°, 40.8°, 49.9°, 54.2°, 62.4°, and 63.9°) in the sorbents [13], which confirms that the main component of all the samples is α-Fe_2O_3. It also can be inferred that the base or acid treatment did not destroy the bulk structure of the sorbents while only the surface acidity was modified.

The breakthrough capacity of the sorbent was tested to illustrate its sulfur removal efficiency. As can be seen in Fig. 3, the sulfur capacity

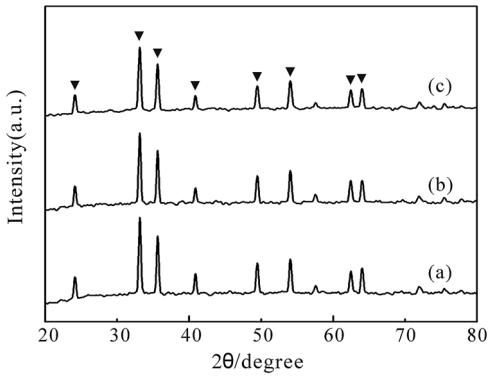

Figure 2. XRD patterns of (a) acid-treated sorbent, (b) iron oxide sorbent, and (c) base-treated sorbent.

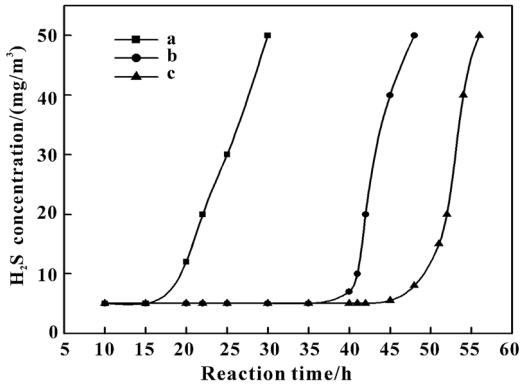

Figure 3. H_2S breakthrough curves of different sorbents: (a) acid-treated sorbent, (b) iron oxide sorbent, and (c) base-treated sorbent.

of the base-treated sorbent is higher than the other two sorbents. By calculation, the sulfur capacity of the base-treated sorbent is 12.2% (wt), while the sulfur capacities of the iron oxide sorbent and acid-treated sorbent are only 10.0 and 5.1% (wt), respectively. Therefore, it can be concluded that the base-treated sorbent shows higher sulfur capacity than both the untreated and acid-treated sorbents for the H_2S removal reaction. The higher activity of the base-treated sorbent is due to the surface basic sites present on the sorbent.

To investigate the effect of surface acid–base property on the H_2S removal reaction, the FT-IR spectra of the exhausted sorbents are also performed (Fig. 4). The band at 3440 cm^{-1}, due to the adsorbed H_2O, is present in the exhausted sorbents. The bands at 1650 and 1410 cm^{-1} are ascribed to the symmetric and asymmetric stretching vibrations of the O–C–O units of HCO_3^- group formed by the reaction of basic hydroxyl groups on the sorbent and CO_2 in air, respectively [14, 15]. By comparing the intensity of the HCO_3^- group in the sorbents, we can find that the corresponding bands in the base-treated sorbent are stronger than that of the other two sorbents, which indicated that base treatment leads to great number of basic hydroxyl groups present on the sorbent. It is noteworthy that the intensity of the bands arising from HCO_3^- group in the acid-treated sorbent is much weaker compared with that of the untreated sorbent, implying that some of the HCO_3^- groups were neutralized by acid during the acid treatment process. The bands at 1020 cm^{-1} (due to SO_3^{2-} groups) [16], 1360 and 1110 cm^{-1} (due to SO_4^{2-} groups) are observed in the spectra [17], indicative of the occurrence of primary H_2S oxidation to form SO_3^{2-} groups and subsequent further oxidation to generate SO_4^{2-} groups.

Indeed, the XPS results (Fig. 5) also show remarkable peaks arising from elemental sulfur (at 163.8 eV), SO_3^{2-} groups (at 164.9 eV) and SO_4^{2-} groups (at 169.4 eV) on the exhausted iron oxide sorbent [18], while no such peaks appears on the corresponding fresh iron oxide sorbent. Therefore, the XPS results also indicate that the oxidation of H_2S into elemental sulfur and further into sulfuric acid and sulfurous acid does take place in the H_2S removal process.

TMPO is a very sensitive probe molecule for determining the relative acid strength of the solid catalyst [19, 20]. In the ^{31}P MAS NMR spectrum (Fig. 6a) of TMPO adsorbed on the base-treated sorbent, only one peak at 43 ppm is observed. After exposing the sample to air for hydration, the intensity of this peak did not decrease, therefore, we unambiguously assign the signal at 43 ppm to physisorbed TMPO in the catalyst [19], which also indicated that no acid site is present on the base-treated sorbent. The ^{31}P MAS NMR spectrum of TMPO adsorbed on the iron oxide sorbent (Fig. 6b) shows two major peaks at 43 ppm (physisorbed TMPO) and 54 ppm (TMPO adsorbed on the weakly acidic –OH groups) [21]. As shown in Fig. 6c, three resonances at 73, 54, and 43 ppm are observed in the ^{31}P NMR spectrum of TMPO adsorbed on the acid-treated sorbent. Similarly, the peak at 43 ppm arises from the physisorbed TMPO. While the peak at 54 ppm is due to TMPO adsorbed on the weakly acidic –OH groups. It is reported that the spectrum of TMPO in contact with H^+ resin reveals a ^{31}P resonance with an isotropic shift of 72 ppm [19]. Therefore, the 73 ppm signal can be ascribed to TMPO adsorbed on the strong Brønsted acid site. This indicates that some strong Brønsted acid sites are present in the acid-treated sorbent. According the reports [21, 22], it is likely that these strong Brønsted acid sites on the sorbent surface are generated in the form of bridging –Fe–OH–Fe– groups in the α-Fe_2O_3 (Scheme 1). Thus, we can conclude that only the weak acid sites (–OH groups) appear on the iron oxide sorbent, while both weak and strong acid sites (–Fe–OH–Fe– groups) arise from the acid-treated sorbent and no acid site is present on the base-treated sorbent.

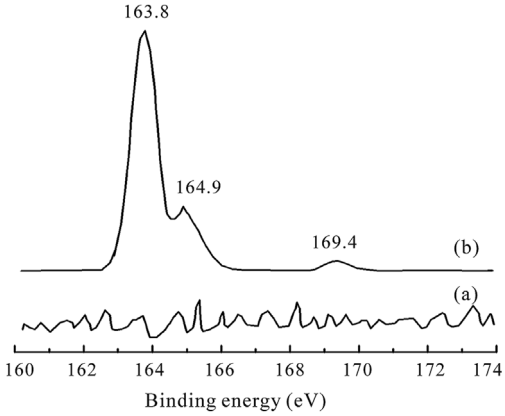

Figure 5. S_{2p} XPS spectra of (a) fresh iron oxide sorbent and (b) exhausted iron oxide sorbent.

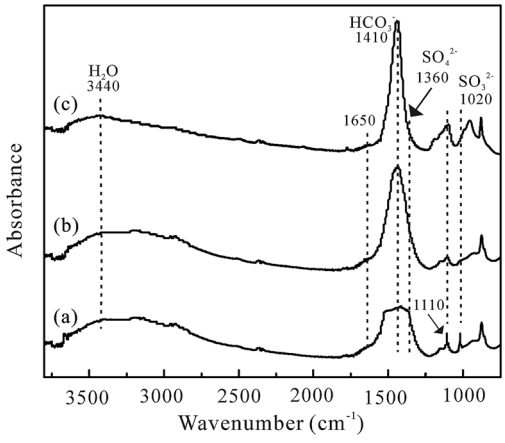

Figure 4. The FT-IR spectra of the exhausted sorbents: (a) acid-treated sorbent, (b) iron oxide sorbent, and (c) base-treated sorbent.

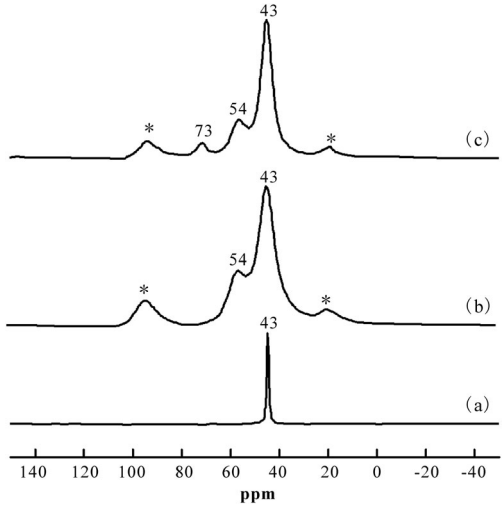

Figure 6. ^{31}P single-pulse MAS NMR spectra (with proton decoupling) of TMPO adsorbed on (a) base-treated sorbent, (b) iron oxide sorbent, and (c) acid-treated sorbent. The asterisk denotes spinning sidebands.

CLEAN Soil Air Water

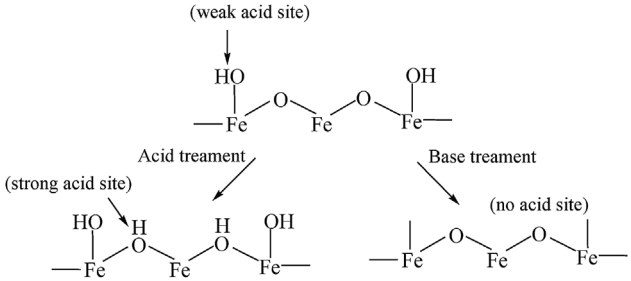

Scheme 1. Acid sites in the iron oxide sorbent, acid-treated sorbent, and base-treated sorbent.

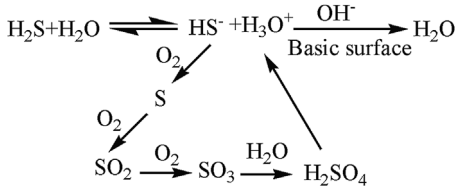

Scheme 2. Proposed pathways of H_2S oxidation on the sorbent surface.

Surface pH and sulfur capability were measured to investigate its surface acid–base property function during the H_2S removal reaction (Tab. 2). The decrease of the surface pH between the fresh and exhausted acid-treated sorbent is much higher than those of iron oxide sorbent and base-treated sorbent. Based on FT-IR and surface pH characterization, we can conclude that sulfuric acid or sulfurous acid formed from the H_2S oxidation reaction increases the surface acidity of the exhausted sorbents compared with the corresponding fresh sorbents. The base-treated sorbent exhibits higher H_2S removal activity, while its surface pH decrease relative slightly, indicating that the basic hydroxyl groups suppress the formation of the acidic species (sulfuric acid and sulfurous acid).

The H_2S oxidation reaction requires the basic surface environment, which promotes the dissociation of H_2S to H_2S ions [23], and then SH^- will further dissociate into S^{2-}. Subsequently, S^{2-} will be converted into the ferric sulfide with α-Fe_2O_3. Hence, the formation of SH^- and S^{2-} is the first step of H_2S removal. The role of α-Fe_2O_3 is to consume the S^{2-} anions from the first step, and then the whole H_2S removal reaction will be completed. Thus, the surface acid–base property of the sorbents plays a significant role in the removal of H_2S. A large number of basic hydroxyl groups existing on the surface of the base-treated sorbent lead to adsorb H_2S molecules more efficiently. The H_2S molecules were first dissociated into H_2S ions, and then these H_2S ions were oxidized into elemental sulfur. These new-formed sulfur atoms are susceptible to further oxidized into SO_2 and SO_3 [24]. As all known, sulfuric acid and sulfurous acid will be easily formed when these sulfur oxides meet with water (Scheme 2). Sulfuric acid and sulfurous acid with strong acidity are unfavorable for the H_2S adsorption on the surface of the sorbent. Nevertheless, in the case of the base-treated sorbent, the basic hydroxyl groups will suspend the acidification effect on the sorbent arising from sulfuric acid and sulfurous acid. For the acid-treated sorbent no basic hydroxyl group exists on its surface, which will remarkably decreases its surface pH. Hence, the activity loss is mainly due to the gradual oxidation of H_2S into elemental sulfur and further into the sulfuric acid and sulfurous acid with time on stream on the surface of the sorbent. As a low cost and widely used sorbent, the sulfur capacity of the iron oxide sorbent is relatively lower than that of activated carbon, zeolites, and other metal based sorbents [2–4]. Thus, the improvement of sulfur capacity will greatly stimulate its application. We found that the basic environment in base-treated iron oxide sorbent results in the higher desulfurization activity and we also gave the clear mechanism based on the experimental evidence. Our findings can be used as the specifications of iron oxide sorbent application for H_2S odor removal.

4 Concluding remarks

In summary, the iron oxide sorbents with different surface acid–base properties were prepared by acid and base modification. The surface acid–base properties and activity of the H_2S odor removal were characterized by surface pH, FT-IR, XPS, and solid-state NMR spectroscopy. The characterization results show that the activity of H_2S removal relies on the surface acid–base characteristics of the iron oxide sorbents. The basic sites in base-treated iron oxide sorbent significantly increase the H_2S removal activity by suppressing the formation of H_2SO_4 or H_2SO_3 during the desulfurization process. While the activity loss of the acid-treated iron oxide sorbent is mainly due to the gradual oxidation of H_2S into elemental sulfur and further into the sulfuric acid and sulfurous acid with time on stream. The detailed information about the role of acid–base property in the sorbent will help us to prepare novel sorbent for more effective H_2S odor removal.

Acknowledgments

This work was supported by grants from the Science and Technology Plan of Wuhan (201060723317), the School Found of WUST (2010XZ012), and the Open Fund of Research Center of Green Manufacturing and Energy-Saving & Emission Reduction Technology in WUST (B1014).

The authors have declared no conflict of interest.

References

[1] S. Asaoka, H. Okamura, R. Morisawa, H. Murakami, K. Fukushi, T. Okajima, M. Katayama, et al., Removal of Hydrogen Sulfide Using Carbonated Steel Slag, *Chem. Eng. J.* **2013**, *228*, 843–849.

Table 2. Comparison of surface pH and sulfur capability of the sorbents

Sorbents	pH fresh sorbent	pH exhausted sorbent	ΔpH	Sulfur capability (wt%)
Acid-treated sorbent	6.20	4.90	1.30	5.1
Iron oxide sorbent	7.56	6.50	1.06	10.0
Base-treated sorbent	8.50	7.52	0.98	12.2

ΔpH = pH (fresh sorbents) – pH (exhausted sorbents).

[2] H. Fang, J. Zhao, Y. Fang, J. Huang, Y. Wang, Selective Oxidation of Hydrogen Sulfide to Sulfur over Activated Carbon-Supported Metal Oxides, *Fuel* **2013**, *108*, 143–148.

[3] K. V. Bineesh, M. Kim, G. Lee, M. Selvaraj, D. Park, Catalytic Performance of Vanadia-Doped Alumina-Pillared Clay for Selective Oxidation of H_2S, *Appl. Clay Sci.* **2013**, *74*, 127–134.

[4] S. Yasyerli, G. Dogu, I. Ar, T. Dogu, Dynamic Analysis of Removal and Selective Oxidation of H_2S to Elemental Sulfur over Cu–V and Cu–V–Mo Mixed Oxides in a Fixed Bed Reactor, *Chem. Eng. Sci.* **2004**, *59*, 4001–4009.

[5] M. Seredych, T. J. Bandosz, Sewage Sludge as a Single Precursor for Development of Composite Adsorbents/Catalysts, *Chem. Eng. J.* **2007**, *128*, 59–67.

[6] H. Duan, R. Yan, L. C. Koe, X. Wang, Combined Effect of Adsorption and Biodegradation of Biological Activated Carbon on H_2S Biotrickling Filtration, *Chemosphere* **2007**, *66*, 1684–1691.

[7] Q. Chen, J. Wang, X. Liu, X. Zhao, W. Qiao, D. Long, L. Ling, Alkaline Carbon Nanotubes as Effective Catalysts for H_2S Oxidation, *Carbon* **2011**, *49*, 3773–3780.

[8] R. Wang, Investigation on a New Liquid Redox Method for H_2S Removal and Sulfur Recovery with Heteropoly Compound, *Sep. Purif. Technol.* **2003**, *31*, 111–121.

[9] A. Bagreev, S. Katikaneni, S. Parab, T. J. Bandosz, Desulfurization of Digester Gas: Prediction of Activated Carbon Bed Performance at Low Concentrations of Hydrogen Sulfide, *Catal. Today* **2005**, *99*, 329–337.

[10] H. Wang, D. Wang, K. T. Chuang, A Sulfur Removal and Disposal Process through H_2S Adsorption and Regeneration: Breakthrough Behaviour Investigation, *Process Saf. Environ. Prot.* **2011**, *89*, 53–60.

[11] R. B. Slimane, J. Abbasian, Regenerable Mixed Metal Oxide Sorbents for Coal Gas Desulfurization at Moderate Temperatures, *Adv. Environ. Res.* **2000**, *4*, 147–162.

[12] F. Adib, A. Bagreev, T. J. Bandosz, Analysis of the Relationship between H_2S Removal Capacity and Surface Properties of Unimpregnated Activated Carbons, *Environ. Sci. Technol.* **2000**, *34*, 686–692.

[13] S. T. Navale, D. K. Bandgar, S. R. Nalage, G. D. Khuspe, M. A. Chougule, Y. D. Kolekar, S. Shashwati, et al., Synthesis of Fe_2O_3 Nanoparticles for Nitrogen Dioxide Gas Sensing Applications, *Ceram. Int.* **2013**, *39*, 6453–6460.

[14] R. L. Frost, S. J. Palmer, Infrared and Infrared Emission Spectroscopy of Nesquehonite $Mg(OH)(HCO_3)\cdot 2\,H_2O$ – Implications for the Formula of Nesquehonite, *Spectrochim. Acta, Part A* **2011**, *78*, 1255–1260.

[15] L. Zhao, X. Li, C. Hao, C. L. Raston, SO_2 Adsorption and Transformation on Calcined NiAl Hydrotalcite-Like Compounds Surfaces: An *in Situ* FTIR and DFT Study, *Appl. Catal., B* **2012**, *117–118*, 339–345.

[16] A. L. Goodman, P. Li, C. R. Usher, Heterogeneous Uptake of Sulfur Dioxide on Aluminum and Magnesium Oxide Particles, *J. Phys. Chem. A* **2001**, *105*, 6109–6120.

[17] T. H. Ko, H. Chu, Spectroscopic Study on Sorption of Hydrogen Sulfide by Means of Red Soil, *Spectrochim. Acta, Part A* **2005**, *61*, 2253–2259.

[18] E. F. Rackiewicz, A. W. Peters, R. F. Wormsbecher, Characterization of Acid Sites in Zeolitic and Other Inorganic Systems Using Solid-State ^{31}P NMR of the Probe Molecule Trimethylphosphine Oxide, *J. Phys. Chem. B* **1998**, *102*, 2890–2896.

[19] J. F. Haw, J. H. Zhang, K. Shimizu, NMR and Theoretical Study of Acidity Probes on Sulfated Zirconia Catalysts, *J. Am. Chem. Soc.* **2000**, *122*, 12561–12570.

[20] Q. Zhao, W. Chen, S. Huang, Y. Wu, H. Lee, S. Liu, Discernment and Quantification of Internal and External Acid Sites on Zeolites, *J. Phys. Chem. B* **2002**, *106*, 4462–4469.

[21] D. Zeng, S. Liu, G. Wang, H. Chen, J. Xu, F. Deng, Effect of Surface Acid Properties of Modified VO_x/Al_2O_3 Catalysts on Methanol Selective Oxidation, *Catal. Lett.* **2013**, *143*, 624–629.

[22] J. Xu, A. Zheng, J. Yang, Y. Su, J. Wang, D. Zeng, M. Zhang, et al., Acidity of Mesoporous MoO_x/ZrO_2 and WO_x/ZrO_2 Materials: A Combined Solid-State NMR and Theoretical Calculation Study, *J. Phys. Chem. B* **2006**, *110*, 10662–10671.

[23] T. J. Bandosz, On the Adsorption/Oxidation of Hydrogen Sulfide on Activated Carbons at Ambient Temperatures, *J. Colloid Interface Sci.* **2002**, *246*, 1–20.

[24] A. Bagreev, H. Rahman, T. J. Bandosz, Study of H_2S Adsorption and Water Regeneration of Spent Coconut-Based Activated Carbon, *Environ. Sci. Technol.* **2000**, *34*, 4587–4592.